

Cross sections for inelastic $K+\phi$ scattering

Yi-Hao Pan and Xiao-Ming Xu¹

¹Department of Physics, Shanghai University, Baoshan, Shanghai 200444, China

Abstract

In the first Born approximation we study the reactions $K\phi \rightarrow \pi K$, ρK , πK^* , and ρK^* with quark-antiquark annihilation and creation. Transition amplitudes are derived with the development in spherical harmonics of the relative-motion wave functions of the two initial mesons and of the two final mesons so that parity is conserved and the total angular momentum of the final mesons equals the one of the initial mesons. Unpolarized cross sections are calculated from the transition amplitudes that also contain mesonic quark-antiquark relative-motion wave functions and transition potentials for quark-antiquark annihilation and creation. Notable temperature dependence of the cross sections is shown. While the cross sections for $K\phi \rightarrow \rho K$, $K\phi \rightarrow \pi K^*$, and $K\phi \rightarrow \rho K^*$ may be of the millibarn scale, the cross section for $K\phi \rightarrow \pi K$ is very small.

Keywords: meson-meson scattering, quark-antiquark annihilation and creation, quark potential model.

PACS: 25.75.-q; 24.85.+p; 12.38.Mh

I. INTRODUCTION

Since enhanced ϕ yield was suggested as a signature for the formation of quark-gluon plasmas [1,2], many measurements on ϕ mesons have been made in relativistic heavy-ion collisions such as Au-Au collisions at the BNL Relativistic Heavy Ion Collider [3–11] or Pb-Pb collisions at the CERN Large Hadron Collider [12–15]. Measured ratios like ϕ/π , ϕ/K , and Ω/ϕ show enhancement of ϕ mesons produced in relativistic heavy-ion collisions relative to $p+p$ collisions. This indicates that strange quarks and strange antiquarks are produced in parton-parton scattering in initial nucleus-nucleus collisions and deconfined matter. Combination of a strange quark and a strange antiquark forms a ϕ meson at hadronization of the quark-gluon plasma. The ϕ meson in collisions with hadrons in hadronic matter may be broken, and this changes the ϕ yield. For example, the ϕ nuclear modification factor as a function of transverse momentum is smaller than 1 for central and midcentral Au-Au collisions at the center-of-mass energy per nucleon-nucleon pair $\sqrt{s_{NN}} = 200$ GeV [3,6] and for central and midcentral Pb-Pb collisions at $\sqrt{s_{NN}} = 2.76$ TeV [13]. Therefore, studying inelastic hadron- ϕ scattering is a fundamental issue in relativistic heavy-ion collisions.

Hadron- ϕ reactions can be studied in hadron degrees of freedom [16–22] or quark degrees of freedom [23,24]. Starting from an effective meson Lagrangian, Feynman diagrams with one-kaon exchange were considered, and squared invariant amplitudes for $\pi\phi \rightarrow K\bar{K}^* + K^*\bar{K}$, $\rho\phi \rightarrow K\bar{K}$, and $\phi\phi \rightarrow K\bar{K}$ were provided in Ref. [17]. Using a Lagrangian that is based on an effective theory in which vector mesons are identified as the dynamical gauge bosons of the hidden $U(3)_V$ local symmetry in the $U(3)_L \times U(3)_R/U(3)_V$ nonlinear sigma model, large cross sections for $K^*\phi \rightarrow \pi K$ and $K\phi \rightarrow \pi K^*$ are shown in Ref. [22]. With a $\pi\phi\rho$ coupling cross sections for $\phi N \rightarrow \pi N$, $\phi N \rightarrow \rho N$, and $\phi N \rightarrow \pi\Delta$ were obtained in Ref. [20]. With a $N\Lambda K$ coupling cross sections for $\phi N \rightarrow K\Lambda$ are shown to be much larger than those for $\phi N \rightarrow \pi N$, $\phi N \rightarrow \rho N$, and $\phi N \rightarrow \pi\Delta$. Experimental efforts to extract the $\phi + N$ total cross section from $d(\gamma, pK^+K^-)n$ have been made by the CLAS Collaboration [25]. The $\phi + N$ cross section may lead to a difference in ϕ

production between π^- -induced reactions on C and W targets [26]. Inelastic $\pi + \phi$ scattering and inelastic $\rho + \phi$ scattering were studied in Ref. [23] in the quark interchange mechanism [27, 28]. Adopting temperature dependence in a quark potential, mesonic quark-antiquark wave functions, and meson masses, prominent temperature-dependent cross sections for the inelastic $\pi + \phi$ and $\rho + \phi$ scattering in hadronic matter were obtained [23]. Besides pions and rho mesons, kaons in hadronic matter also interact with ϕ mesons. However, quark-level study of inelastic $K + \phi$ scattering has not been done. Moreover, temperature dependence of the inelastic $K + \phi$ scattering is unexplored both experimentally and theoretically. Therefore, the present work aims to study the inelastic $K + \phi$ scattering and their temperature dependence.

Some meson-meson reactions may be dominated by the process where a quark and an antiquark annihilate into a gluon and subsequently the gluon creates another quark-antiquark pair. Such quark-antiquark annihilation and creation has been used in Refs. [29, 30] to obtain unpolarized cross sections for the reactions: $\pi\pi \rightarrow \rho\rho$, $K\bar{K} \rightarrow K^*\bar{K}^*$, $K\bar{K}^* \rightarrow K^*\bar{K}^*$, $K^*\bar{K} \rightarrow K^*\bar{K}^*$, $\pi\pi \rightarrow K\bar{K}$, $\pi\rho \rightarrow K\bar{K}^*$, $\pi\rho \rightarrow K^*\bar{K}$, $K\bar{K} \rightarrow \rho\rho$, $K\bar{K} \rightarrow K\bar{K}^*$, $K\bar{K} \rightarrow K^*\bar{K}$, $\pi K \rightarrow \pi K^*$, $\pi K \rightarrow \rho K$, $\pi\pi \rightarrow K\bar{K}^*$, $\pi\pi \rightarrow K^*\bar{K}$, $\pi\pi \rightarrow K^*\bar{K}^*$, $\pi\rho \rightarrow K\bar{K}$, $\pi\rho \rightarrow K^*\bar{K}^*$, $\rho\rho \rightarrow K^*\bar{K}^*$, $K\bar{K}^* \rightarrow \rho\rho$, and $K^*\bar{K} \rightarrow \rho\rho$. The s quark (or the \bar{s} antiquark) of a kaon may annihilate with the \bar{s} antiquark (or the s quark) of a ϕ meson to produce a gluon, and subsequently the gluon splits into a $u\bar{u}$ or $d\bar{d}$ pair. The $u\bar{u}$ or $d\bar{d}$ pair combines with spectator constituents of the K and ϕ mesons to form two mesons that are not ϕ mesons. Quark-antiquark annihilation and creation thus leads to inelastic $K + \phi$ scattering. By contrast quark interchange does not cause inelastic $K + \phi$ scattering. The mechanism that governs the inelastic $K + \phi$ scattering completely differs from the mechanism that governs the inelastic $\pi + \phi$ and $\rho + \phi$ scattering. Therefore, with quark-antiquark annihilation and creation in the first Born approximation, in the present work we study the reactions: $K\phi \rightarrow \pi K$, $K\phi \rightarrow \rho K$, $K\phi \rightarrow \pi K^*$, and $K\phi \rightarrow \rho K^*$.

This paper is organized as follows. In the next section we derive transition-amplitude formulas for 2-to-2 meson-meson scattering that are driven by quark-antiquark annihilation and creation. Numerical results and relevant discussions are given in Sec. III. A

summary is in the last section.

II. FORMALISM

The reaction $A(q_1\bar{q}_1) + B(q_2\bar{q}_2) \rightarrow C(q_3\bar{q}_1) + D(q_2\bar{q}_4)$ ($A(q_1\bar{q}_1) + B(q_2\bar{q}_2) \rightarrow C(q_1\bar{q}_4) + D(q_3\bar{q}_2)$) takes place due to that quark q_1 (q_2) and antiquark \bar{q}_2 (\bar{q}_1) in the initial mesons annihilate into a gluon and subsequently the gluon creates quark q_3 and antiquark \bar{q}_4 . The two processes $q_1 + \bar{q}_2 \rightarrow q_3 + \bar{q}_4$ and $\bar{q}_1 + q_2 \rightarrow q_3 + \bar{q}_4$ give rise to the two transition potentials $V_{aq_1\bar{q}_2}$ and $V_{a\bar{q}_1q_2}$, respectively. Denote by E_i and \vec{P}_i (E_f and \vec{P}_f) the total energy and the total momentum of the two initial (final) mesons, respectively. Let E_A (E_B , E_C , E_D) be the energy of meson A (B , C , D), and V the volume where every meson wave function is normalized. The S -matrix element for $A + B \rightarrow C + D$ is

$$S_{fi} = \delta_{fi} - (2\pi)^4 i \delta(E_f - E_i) \delta^3(\vec{P}_f - \vec{P}_i) \frac{\mathcal{M}_{aq_1\bar{q}_2} + \mathcal{M}_{a\bar{q}_1q_2}}{V^2 \sqrt{2E_A 2E_B 2E_C 2E_D}}, \quad (1)$$

where $\mathcal{M}_{aq_1\bar{q}_2}$ and $\mathcal{M}_{a\bar{q}_1q_2}$ are the transition amplitudes given by

$$\begin{aligned} \mathcal{M}_{aq_1\bar{q}_2} &= \frac{(m_{q_3} + m_{\bar{q}_1})^3}{m_{\bar{q}_1}^3} \sqrt{2E_A 2E_B 2E_C 2E_D} \\ &\times \int d\vec{r}_{q_1\bar{q}_1} d\vec{r}_{q_2\bar{q}_4} d\vec{r}_{q_3\bar{q}_1, q_2\bar{q}_4} \psi_{CD}^+ V_{aq_1\bar{q}_2} \\ &\times \psi_{AB} e^{i\vec{p}_{q_1\bar{q}_1, q_2\bar{q}_2} \cdot \vec{r}_{q_1\bar{q}_1, q_2\bar{q}_2} - i\vec{p}_{q_3\bar{q}_1, q_2\bar{q}_4} \cdot \vec{r}_{q_3\bar{q}_1, q_2\bar{q}_4}}, \end{aligned} \quad (2)$$

$$\begin{aligned} \mathcal{M}_{a\bar{q}_1q_2} &= \frac{(m_{q_1} + m_{\bar{q}_4})^3}{m_{q_1}^3} \sqrt{2E_A 2E_B 2E_C 2E_D} \\ &\times \int d\vec{r}_{q_1\bar{q}_1} d\vec{r}_{q_3\bar{q}_2} d\vec{r}_{q_1\bar{q}_4, q_3\bar{q}_2} \psi_{CD}^+ V_{a\bar{q}_1q_2} \\ &\times \psi_{AB} e^{i\vec{p}_{q_1\bar{q}_1, q_2\bar{q}_2} \cdot \vec{r}_{q_1\bar{q}_1, q_2\bar{q}_2} - i\vec{p}_{q_1\bar{q}_4, q_3\bar{q}_2} \cdot \vec{r}_{q_1\bar{q}_4, q_3\bar{q}_2}}, \end{aligned} \quad (3)$$

where m_{q_1} ($m_{\bar{q}_1}$, m_{q_3} , $m_{\bar{q}_4}$) is the mass of q_1 (\bar{q}_1 , q_3 , \bar{q}_4); \vec{r}_{ab} the relative coordinate of constituents a and b ; $\vec{r}_{q_1\bar{q}_1, q_2\bar{q}_2}$ ($\vec{r}_{q_3\bar{q}_1, q_2\bar{q}_4}$, $\vec{r}_{q_1\bar{q}_4, q_3\bar{q}_2}$) the relative coordinate of $q_1\bar{q}_1$ and $q_2\bar{q}_2$ ($q_3\bar{q}_1$ and $q_2\bar{q}_4$, $q_1\bar{q}_4$ and $q_3\bar{q}_2$); $\vec{p}_{q_1\bar{q}_1, q_2\bar{q}_2}$ ($\vec{p}_{q_3\bar{q}_1, q_2\bar{q}_4}$, $\vec{p}_{q_1\bar{q}_4, q_3\bar{q}_2}$) the relative momentum of $q_1\bar{q}_1$ and $q_2\bar{q}_2$ ($q_3\bar{q}_1$ and $q_2\bar{q}_4$, $q_1\bar{q}_4$ and $q_3\bar{q}_2$); ψ_{AB} (ψ_{CD}) the wave function of mesons A and B (C and D), and ψ_{AB}^+ (ψ_{CD}^+) the Hermitean conjugate of ψ_{AB} (ψ_{CD}). The wave function of mesons A and B is

$$\psi_{AB} = \phi_{Acolor} \phi_{Bcolor} \phi_{Arel} \phi_{Brel} \chi_{S_A S_{Az}} \chi_{S_B S_{Bz}} \varphi_{AB flavor}, \quad (4)$$

and the wave function of mesons C and D is

$$\psi_{CD} = \phi_{C\text{color}} \phi_{D\text{color}} \phi_{C\text{rel}} \phi_{D\text{rel}} \chi_{S_C S_{Cz}} \chi_{S_D S_{Dz}} \varphi_{CD\text{flavor}}, \quad (5)$$

where S_A (S_B , S_C , S_D) is the spin of meson A (B , C , D) with its magnetic projection quantum number S_{Az} (S_{Bz} , S_{Cz} , S_{Dz}); $\phi_{A\text{color}}$ ($\phi_{B\text{color}}$, $\phi_{C\text{color}}$, $\phi_{D\text{color}}$), $\phi_{A\text{rel}}$ ($\phi_{B\text{rel}}$, $\phi_{C\text{rel}}$, $\phi_{D\text{rel}}$), and $\chi_{S_A S_{Az}}$ ($\chi_{S_B S_{Bz}}$, $\chi_{S_C S_{Cz}}$, $\chi_{S_D S_{Dz}}$) are the color wave function, the quark-antiquark relative-motion wave function, and the spin wave function of meson A (B , C , D), respectively; $\varphi_{AB\text{flavor}}$ ($\varphi_{CD\text{flavor}}$) is the flavor wave function of mesons A and B (C and D).

The development in spherical harmonics of the relative-motion wave function of mesons A and B (aside from a normalization constant) is given by

$$\begin{aligned} e^{i\vec{p}_{q_1\bar{q}_1,q_2\bar{q}_2} \cdot \vec{r}_{q_1\bar{q}_1,q_2\bar{q}_2}} &= 4\pi \sum_{L_i=0}^{\infty} \sum_{M_i=-L_i}^{L_i} i^{L_i} j_{L_i}(|\vec{p}_{q_1\bar{q}_1,q_2\bar{q}_2}| r_{q_1\bar{q}_1,q_2\bar{q}_2}) \\ &\times Y_{L_i M_i}^*(\hat{p}_{q_1\bar{q}_1,q_2\bar{q}_2}) Y_{L_i M_i}(\hat{r}_{q_1\bar{q}_1,q_2\bar{q}_2}), \end{aligned} \quad (6)$$

and the development in spherical harmonics of the relative-motion wave function of mesons C and D leads to

$$\begin{aligned} e^{-i\vec{p}_{q_3\bar{q}_1,q_2\bar{q}_4} \cdot \vec{r}_{q_3\bar{q}_1,q_2\bar{q}_4}} &= 4\pi \sum_{L_f=0}^{\infty} \sum_{M_f=-L_f}^{L_f} i^{L_f} (-1)^{L_f} j_{L_f}(|\vec{p}_{q_3\bar{q}_1,q_2\bar{q}_4}| r_{q_3\bar{q}_1,q_2\bar{q}_4}) \\ &\times Y_{L_f M_f}^*(\hat{p}_{q_3\bar{q}_1,q_2\bar{q}_4}) Y_{L_f M_f}(\hat{r}_{q_3\bar{q}_1,q_2\bar{q}_4}), \end{aligned} \quad (7)$$

in $\mathcal{M}_{aq_1\bar{q}_2}$, and

$$\begin{aligned} e^{-i\vec{p}_{q_1\bar{q}_4,q_3\bar{q}_2} \cdot \vec{r}_{q_1\bar{q}_4,q_3\bar{q}_2}} &= 4\pi \sum_{L_f=0}^{\infty} \sum_{M_f=-L_f}^{L_f} i^{L_f} (-1)^{L_f} j_{L_f}(|\vec{p}_{q_1\bar{q}_4,q_3\bar{q}_2}| r_{q_1\bar{q}_4,q_3\bar{q}_2}) \\ &\times Y_{L_f M_f}^*(\hat{p}_{q_1\bar{q}_4,q_3\bar{q}_2}) Y_{L_f M_f}(\hat{r}_{q_1\bar{q}_4,q_3\bar{q}_2}), \end{aligned} \quad (8)$$

in $\mathcal{M}_{a\bar{q}_1q_2}$, where $Y_{L_i M_i}$ ($Y_{L_f M_f}$) are the spherical harmonics with the orbital-angular-momentum quantum number L_i (L_f) and the magnetic projection quantum number M_i (M_f), j_{L_i} and j_{L_f} are the spherical Bessel functions, and $\hat{p}_{q_1\bar{q}_1,q_2\bar{q}_2}$ ($\hat{p}_{q_3\bar{q}_1,q_2\bar{q}_4}$, $\hat{p}_{q_1\bar{q}_4,q_3\bar{q}_2}$, $\hat{r}_{q_1\bar{q}_1,q_2\bar{q}_2}$, $\hat{r}_{q_3\bar{q}_1,q_2\bar{q}_4}$, $\hat{r}_{q_1\bar{q}_4,q_3\bar{q}_2}$) denotes the polar angles of $\vec{p}_{q_1\bar{q}_1,q_2\bar{q}_2}$ ($\vec{p}_{q_3\bar{q}_1,q_2\bar{q}_4}$, $\vec{p}_{q_1\bar{q}_4,q_3\bar{q}_2}$, $\vec{r}_{q_1\bar{q}_1,q_2\bar{q}_2}$, $\vec{r}_{q_3\bar{q}_1,q_2\bar{q}_4}$, $\vec{r}_{q_1\bar{q}_4,q_3\bar{q}_2}$).

Let χ_{SS_z} ($\chi_{S'S'_z}$) stand for the spin wave function of mesons A and B (C and D), which has the total spin S (S') and its z component S_z (S'_z). The Clebsch-Gordan coefficients $(S_A S_{A_z} S_B S_{B_z} | SS_z)$ relate χ_{SS_z} to $\chi_{S_A S_{A_z}} \chi_{S_B S_{B_z}}$, and $(S_C S_{C_z} S_D S_{D_z} | S' S'_z)$ relate $\chi_{S' S'_z}$ to $\chi_{S_C S_{C_z}} \chi_{S_D S_{D_z}}$.

$$\chi_{S_A S_{A_z}} \chi_{S_B S_{B_z}} = \sum_{S=S_{\min}}^{S_{\max}} \sum_{S_z=-S}^S (S_A S_{A_z} S_B S_{B_z} | SS_z) \chi_{SS_z}, \quad (9)$$

$$\chi_{S_C S_{C_z}} \chi_{S_D S_{D_z}} = \sum_{S'=S'_{\min}}^{S'_{\max}} \sum_{S'_z=-S'}^{S'} (S_C S_{C_z} S_D S_{D_z} | S' S'_z) \chi_{S' S'_z}, \quad (10)$$

where $S_{\min} = |S_A - S_B|$, $S_{\max} = S_A + S_B$, $S'_{\min} = |S_C - S_D|$, and $S'_{\max} = S_C + S_D$. $Y_{L_i M_i}$ and χ_{SS_z} ($Y_{L_f M_f}$ and $\chi_{S' S'_z}$) are coupled to the wave function $\varphi_{JJ_z}^{\text{in}}$ ($\varphi_{J'J'_z}^{\text{final}}$) which has the total angular momentum J (J') of mesons A and B (C and D) and its z component J_z (J'_z),

$$Y_{L_i M_i} \chi_{SS_z} = \sum_{J=J_{\min}}^{J_{\max}} \sum_{J_z=-J}^J (L_i M_i SS_z | JJ_z) \varphi_{JJ_z}^{\text{in}}, \quad (11)$$

$$Y_{L_f M_f} \chi_{S' S'_z} = \sum_{J'=J'_{\min}}^{J'_{\max}} \sum_{J'_z=-J'}^{J'} (L_f M_f S' S'_z | J' J'_z) \varphi_{J'J'_z}^{\text{final}}, \quad (12)$$

where $J_{\min} = |L_i - S|$, $J_{\max} = L_i + S$, $J'_{\min} = |L_f - S'|$, and $J'_{\max} = L_f + S'$. $(L_i M_i SS_z | JJ_z)$ and $(L_f M_f S' S'_z | J' J'_z)$ are the Clebsch-Gordan coefficients. It follows from Eqs. (6)-(12) that the transition amplitude given in Eq. (3) becomes

$$\begin{aligned} \mathcal{M}_{a\bar{q}_1 q_2} &= \frac{(m_{q_1} + m_{\bar{q}_4})^3}{m_{q_1}^3} \sqrt{2E_A 2E_B 2E_C 2E_D} (4\pi)^2 \sum_{L_i=0}^{\infty} \sum_{M_i=-L_i}^{L_i} i^{L_i} Y_{L_i M_i}^* (\hat{p}_{q_1 \bar{q}_1, q_2 \bar{q}_2}) \\ &\times \sum_{L_f=0}^{\infty} \sum_{M_f=-L_f}^{L_f} i^{L_f} (-1)^{L_f} Y_{L_f M_f}^* (\hat{p}_{q_1 \bar{q}_4, q_3 \bar{q}_2}) \phi_{C\text{color}}^+ \phi_{D\text{color}}^+ \varphi_{CD\text{flavor}}^+ \\ &\times \int d\vec{r}_{q_1 \bar{q}_1} d\vec{r}_{q_3 \bar{q}_2} d\vec{r}_{q_1 \bar{q}_4, q_3 \bar{q}_2} \phi_{C\text{rel}}^+ \phi_{D\text{rel}}^+ \sum_{S' S'_z} (S_C S_{C_z} S_D S_{D_z} | S' S'_z) \\ &\times \sum_{J' J'_z} (L_f M_f S' S'_z | J' J'_z) \varphi_{J' J'_z}^{\text{final}} V_{a q_1 \bar{q}_2} \sum_{SS_z} (S_A S_{A_z} S_B S_{B_z} | SS_z) \\ &\times \sum_{JJ_z} (L_i M_i SS_z | JJ_z) \varphi_{JJ_z}^{\text{in}} \phi_{A\text{rel}} \phi_{B\text{rel}} \varphi_{AB\text{flavor}} \phi_{A\text{color}} \phi_{B\text{color}} \\ &\times j_{L_i}(|\vec{p}_{q_1 \bar{q}_1, q_2 \bar{q}_2}| r_{q_1 \bar{q}_1, q_2 \bar{q}_2}) j_{L_f}(|\vec{p}_{q_1 \bar{q}_4, q_3 \bar{q}_2}| r_{q_1 \bar{q}_4, q_3 \bar{q}_2}). \end{aligned} \quad (13)$$

Conservation of the total angular momentum implies that J equals J' and J_z equals J'_z .

This leads to

$$\begin{aligned}
\mathcal{M}_{a\bar{q}_1 q_2} &= \frac{(m_{q_1} + m_{\bar{q}_4})^3}{m_{q_1}^3} \sqrt{2E_A 2E_B 2E_C 2E_D} (4\pi)^2 \sum_{L_i=0}^{\infty} \sum_{M_i=-L_i}^{L_i} i^{L_i} Y_{L_i M_i}^* (\hat{p}_{q_1 \bar{q}_1, q_2 \bar{q}_2}) \\
&\times \sum_{L_f=0}^{\infty} \sum_{M_f=-L_f}^{L_f} i^{L_f} (-1)^{L_f} Y_{L_f M_f}^* (\hat{p}_{q_1 \bar{q}_4, q_3 \bar{q}_2}) \phi_{C\text{color}}^+ \phi_{D\text{color}}^+ \phi_{CD\text{flavor}}^+ \\
&\times \int d\vec{r}_{q_1 \bar{q}_1} d\vec{r}_{q_3 \bar{q}_2} d\vec{r}_{q_1 \bar{q}_4, q_3 \bar{q}_2} \phi_{C\text{rel}}^+ \phi_{D\text{rel}}^+ \sum_{S' S'_z} (S_C S_{Cz} S_D S_{Dz} | S' S'_z) \\
&\times \sum_{JJ_z} (L_f M_f S' S'_z | JJ_z) \varphi_{JJ_z}^{\text{final}} V_{a\bar{q}_1 q_2} \sum_{SS_z} (S_A S_{Az} S_B S_{Bz} | SS_z) \\
&\times (L_i M_i SS_z | JJ_z) \varphi_{JJ_z}^{\text{in}} \phi_{A\text{rel}} \phi_{B\text{rel}} \varphi_{AB\text{flavor}} \phi_{A\text{color}} \phi_{B\text{color}} \\
&\times j_{L_i}(|\vec{p}_{q_1 \bar{q}_1, q_2 \bar{q}_2} | \vec{r}_{q_1 \bar{q}_1, q_2 \bar{q}_2}) j_{L_f}(|\vec{p}_{q_1 \bar{q}_4, q_3 \bar{q}_2} | \vec{r}_{q_1 \bar{q}_4, q_3 \bar{q}_2}). \tag{14}
\end{aligned}$$

Using the relation

$$\varphi_{JJ_z}^{\text{in}} = \sum_{\bar{M}_i \bar{S}_z} (L_i \bar{M}_i S \bar{S}_z | JJ_z) Y_{L_i \bar{M}_i} \chi_{S \bar{S}_z}, \tag{15}$$

$$\varphi_{JJ_z}^{\text{final}} = \sum_{\bar{M}_f \bar{S}'_z} (L_f \bar{M}_f S' \bar{S}'_z | JJ_z) Y_{L_f \bar{M}_f} \chi_{S' \bar{S}'_z}, \tag{16}$$

where $(L_i \bar{M}_i S \bar{S}_z | JJ_z)$ and $(L_f \bar{M}_f S' \bar{S}'_z | JJ_z)$ are the Clebsch-Gordan coefficients, we get

$$\begin{aligned}
\mathcal{M}_{a\bar{q}_1 q_2} &= \frac{(m_{q_1} + m_{\bar{q}_4})^3}{m_{q_1}^3} \sqrt{2E_A 2E_B 2E_C 2E_D} (4\pi)^2 \sum_{L_i=0}^{\infty} \sum_{M_i=-L_i}^{L_i} i^{L_i} Y_{L_i M_i}^* (\hat{p}_{q_1 \bar{q}_1, q_2 \bar{q}_2}) \\
&\times \sum_{L_f=0}^{\infty} \sum_{M_f=-L_f}^{L_f} i^{L_f} (-1)^{L_f} Y_{L_f M_f}^* (\hat{p}_{q_1 \bar{q}_4, q_3 \bar{q}_2}) \sum_{S' S'_z} (S_C S_{Cz} S_D S_{Dz} | S' S'_z) \\
&\times \sum_{JJ_z} (L_f M_f S' S'_z | JJ_z) \sum_{\bar{M}_f \bar{S}'_z} (L_f \bar{M}_f S' \bar{S}'_z | JJ_z) \sum_{SS_z} (S_A S_{Az} S_B S_{Bz} | SS_z) \\
&\times (L_i M_i SS_z | JJ_z) \sum_{\bar{M}_i \bar{S}_z} (L_i \bar{M}_i S \bar{S}_z | JJ_z) \phi_{C\text{color}}^+ \phi_{D\text{color}}^+ \phi_{CD\text{flavor}}^+ \chi_{S' \bar{S}'_z}^+ \\
&\times \int d\vec{r}_{q_1 \bar{q}_1} d\vec{r}_{q_3 \bar{q}_2} d\vec{r}_{q_1 \bar{q}_4, q_3 \bar{q}_2} j_{L_f}(|\vec{p}_{q_1 \bar{q}_4, q_3 \bar{q}_2} | \vec{r}_{q_1 \bar{q}_4, q_3 \bar{q}_2}) Y_{L_f \bar{M}_f}(\hat{r}_{q_1 \bar{q}_4, q_3 \bar{q}_2}) \\
&\times \phi_{C\text{rel}}^+ \phi_{D\text{rel}}^+ V_{a\bar{q}_1 q_2} \phi_{A\text{rel}} \phi_{B\text{rel}} j_{L_i}(|\vec{p}_{q_1 \bar{q}_1, q_2 \bar{q}_2} | \vec{r}_{q_1 \bar{q}_1, q_2 \bar{q}_2}) Y_{L_i \bar{M}_i}(\hat{r}_{q_1 \bar{q}_1, q_2 \bar{q}_2}) \\
&\times \chi_{S \bar{S}_z} \varphi_{AB\text{flavor}} \phi_{A\text{color}} \phi_{B\text{color}}. \tag{17}
\end{aligned}$$

Furthermore, we need the identity

$$j_l(pr) Y_{lm}(\hat{r}) = \int \frac{d^3 p'}{(2\pi)^3} \frac{2\pi^2}{p^2} \delta(p - p') i^l (-1)^l Y_{lm}(\hat{p}') e^{i\vec{p}' \cdot \vec{r}}, \tag{18}$$

which is obtained with the help of $\int_0^\infty j_l(pr)j_l(p'r)r^2dr = \frac{\pi}{2p^2}\delta(p-p')$ [31, 32], and where \hat{r} (\hat{p}') denotes the polar angles of \vec{r} (\vec{p}'). Substituting Eq. (18) in Eq. (17), we get

$$\begin{aligned}
\mathcal{M}_{a\bar{q}_1q_2} = & \frac{(m_{q_1} + m_{\bar{q}_4})^3}{m_{q_1}^3} \sqrt{2E_A 2E_B 2E_C 2E_D} (4\pi)^2 \sum_{L_i=0}^{\infty} \sum_{M_i=-L_i}^{L_i} i^{L_i} Y_{L_i M_i}^* (\hat{p}_{q_1\bar{q}_1, q_2\bar{q}_2}) \\
& \times \sum_{L_f=0}^{\infty} \sum_{M_f=-L_f}^{L_f} i^{L_f} (-1)^{L_f} Y_{L_f M_f}^* (\hat{p}_{q_1\bar{q}_4, q_3\bar{q}_2}) \sum_{S' S'_z} (S_C S_{Cz} S_D S_{Dz} | S' S'_z) \\
& \times \sum_{J J_z} (L_f M_f S' S'_z | J J_z) \sum_{\bar{M}_f \bar{S}'_z} (L_f \bar{M}_f S' \bar{S}'_z | J J_z) \sum_{S S_z} (S_A S_{Az} S_B S_{Bz} | S S_z) \\
& \times (L_i M_i S S_z | J J_z) \sum_{\bar{M}_i \bar{S}_z} (L_i \bar{M}_i S \bar{S}_z | J J_z) \phi_{C\text{color}}^+ \phi_{D\text{color}}^+ \varphi_{CD\text{flavor}}^+ \chi_{S' \bar{S}'_z}^+ \\
& \times \int \frac{d^3 p_{\text{frm}}}{(2\pi)^3} \frac{2\pi^2}{\vec{p}_{q_1\bar{q}_4, q_3\bar{q}_2}^2} \delta(|\vec{p}_{q_1\bar{q}_4, q_3\bar{q}_2}| - |\vec{p}_{\text{frm}}|) i^{L_f} (-1)^{L_f} Y_{L_f \bar{M}_f} (\hat{p}_{\text{frm}}) \\
& \times \int \frac{d^3 p_{\text{irm}}}{(2\pi)^3} \frac{2\pi^2}{\vec{p}_{q_1\bar{q}_1, q_2\bar{q}_2}^2} \delta(|\vec{p}_{q_1\bar{q}_1, q_2\bar{q}_2}| - |\vec{p}_{\text{irm}}|) i^{L_i} (-1)^{L_i} Y_{L_i \bar{M}_i} (\hat{p}_{\text{irm}}) \\
& \times \int d\vec{r}_{q_1\bar{q}_1} d\vec{r}_{q_3\bar{q}_2} d\vec{r}_{q_1\bar{q}_4, q_3\bar{q}_2} \phi_{C\text{rel}}^+ \phi_{D\text{rel}}^+ V_{a\bar{q}_1q_2} \phi_{A\text{rel}} \phi_{B\text{rel}} \\
& \times e^{i\vec{p}_{\text{frm}} \cdot \vec{r}_{q_1\bar{q}_4, q_3\bar{q}_2}} e^{i\vec{p}_{\text{irm}} \cdot \vec{r}_{q_1\bar{q}_1, q_2\bar{q}_2}} \chi_{S \bar{S}_z} \varphi_{AB\text{flavor}} \phi_{A\text{color}} \phi_{B\text{color}}. \tag{19}
\end{aligned}$$

Let \vec{r}_c be the position vector of constituent c . $\phi_{A\text{rel}}$ and $\phi_{B\text{rel}}$ are functions of the relative coordinate of the quark and the antiquark inside mesons A and B , respectively. We take the Fourier transform of $V_{a\bar{q}_1\bar{q}_2}$, $V_{a\bar{q}_1q_2}$, $\phi_{A\text{rel}}$, and $\phi_{B\text{rel}}$:

$$V_{a\bar{q}_1\bar{q}_2}(\vec{r}_{q_3} - \vec{r}_{q_1}) = \int \frac{d^3 k}{(2\pi)^3} V_{a\bar{q}_1\bar{q}_2}(\vec{k}) e^{i\vec{k} \cdot (\vec{r}_{q_3} - \vec{r}_{q_1})}, \tag{20}$$

$$V_{a\bar{q}_1q_2}(\vec{r}_{q_3} - \vec{r}_{q_2}) = \int \frac{d^3 k}{(2\pi)^3} V_{a\bar{q}_1q_2}(\vec{k}) e^{i\vec{k} \cdot (\vec{r}_{q_3} - \vec{r}_{q_2})}, \tag{21}$$

$$\phi_{A\text{rel}}(\vec{r}_{q_1\bar{q}_1}) = \int \frac{d^3 p_{q_1\bar{q}_1}}{(2\pi)^3} \phi_{A\text{rel}}(\vec{p}_{q_1\bar{q}_1}) e^{i\vec{p}_{q_1\bar{q}_1} \cdot \vec{r}_{q_1\bar{q}_1}}, \tag{22}$$

$$\phi_{B\text{rel}}(\vec{r}_{q_2\bar{q}_2}) = \int \frac{d^3 p_{q_2\bar{q}_2}}{(2\pi)^3} \phi_{B\text{rel}}(\vec{p}_{q_2\bar{q}_2}) e^{i\vec{p}_{q_2\bar{q}_2} \cdot \vec{r}_{q_2\bar{q}_2}}. \tag{23}$$

In Eqs. (20)-(21) \vec{k} is the gluon momentum, and in Eqs. (22)-(23) \vec{p}_{ab} is the relative momentum of constituents a and b . In momentum space the normalizations are

$$\int \frac{d^3 p_{q_1\bar{q}_1}}{(2\pi)^3} \phi_{A\text{rel}}^+(\vec{p}_{q_1\bar{q}_1}) \phi_{A\text{rel}}(\vec{p}_{q_1\bar{q}_1}) = 1,$$

$$\int \frac{d^3 p_{q_2\bar{q}_2}}{(2\pi)^3} \phi_{B\text{rel}}^+(\vec{p}_{q_2\bar{q}_2}) \phi_{B\text{rel}}(\vec{p}_{q_2\bar{q}_2}) = 1.$$

The spherical polar coordinates of \vec{p}_{irm} and \vec{p}_{frm} are expressed as $(|\vec{p}_{\text{irm}}|, \theta_{\text{irm}}, \phi_{\text{irm}})$ and $(|\vec{p}_{\text{frm}}|, \theta_{\text{frm}}, \phi_{\text{frm}})$, respectively. Integration over $|\vec{p}_{\text{irm}}|$, $|\vec{p}_{\text{frm}}|$, $\vec{r}_{q_1\bar{q}_1}$, $\vec{r}_{q_3\bar{q}_2}$, and $\vec{r}_{q_1\bar{q}_4, q_3\bar{q}_2}$ in Eq. (19) yields

$$\begin{aligned}
\mathcal{M}_{a\bar{q}_1 q_2} &= \sqrt{2E_A 2E_B 2E_C 2E_D} \sum_{L_i=0}^{\infty} \sum_{M_i=-L_i}^{L_i} Y_{L_i M_i}^* (\hat{p}_{q_1\bar{q}_1, q_2\bar{q}_2}) \\
&\times \sum_{L_f=0}^{\infty} \sum_{M_f=-L_f}^{L_f} (-1)^{L_f} Y_{L_f M_f}^* (\hat{p}_{q_1\bar{q}_4, q_3\bar{q}_2}) \sum_{S' S'_z} (S_C S_{Cz} S_D S_{Dz} | S' S'_z) \\
&\times \sum_{J J_z} (L_f M_f S' S'_z | J J_z) \sum_{\bar{M}_f \bar{S}'_z} (L_f \bar{M}_f S' \bar{S}'_z | J J_z) \sum_{S S_z} (S_A S_{Az} S_B S_{Bz} | S S_z) \\
&\times (L_i M_i S S_z | J J_z) \sum_{\bar{M}_i \bar{S}_z} (L_i \bar{M}_i S \bar{S}_z | J J_z) \phi_{C\text{color}}^+ \phi_{D\text{color}}^+ \phi_{CD\text{flavor}}^+ \chi_{S' \bar{S}'_z}^+ \\
&\times \int d\theta_{\text{frm}} d\phi_{\text{frm}} \sin \theta_{\text{frm}} Y_{L_f \bar{M}_f} (\hat{p}_{\text{frm}}) \int d\theta_{\text{irm}} d\phi_{\text{irm}} \sin \theta_{\text{irm}} Y_{L_i \bar{M}_i} (\hat{p}_{\text{irm}}) \\
&\times \int \frac{d^3 p_{q_1\bar{q}_1}}{(2\pi)^3} \int \frac{d^3 p_{q_2\bar{q}_2}}{(2\pi)^3} \phi_{C\text{rel}}^+ (\vec{p}_{q_1\bar{q}_1} + \frac{m_{q_1}}{m_{q_1} + m_{\bar{q}_1}} \vec{p}_{\text{irm}} + \frac{m_{q_1}}{m_{q_1} + m_{\bar{q}_4}} \vec{p}_{\text{frm}}) \\
&\times \phi_{D\text{rel}}^+ (\vec{p}_{q_2\bar{q}_2} + \frac{m_{\bar{q}_2}}{m_{q_2} + m_{\bar{q}_2}} \vec{p}_{\text{irm}} + \frac{m_{\bar{q}_2}}{m_{q_3} + m_{\bar{q}_2}} \vec{p}_{\text{frm}}) \\
&\times V_{a\bar{q}_1 q_2} [\vec{p}_{q_2\bar{q}_2} - \vec{p}_{q_1\bar{q}_1} - (\frac{m_{q_2}}{m_{q_2} + m_{\bar{q}_2}} - \frac{m_{\bar{q}_1}}{m_{q_1} + m_{\bar{q}_1}}) \vec{p}_{\text{irm}}] \\
&\times \phi_{A\text{rel}} (\vec{p}_{q_1\bar{q}_1}) \phi_{B\text{rel}} (\vec{p}_{q_2\bar{q}_2}) \chi_{S \bar{S}_z} \varphi_{AB\text{flavor}} \phi_{A\text{color}} \phi_{B\text{color}}, \tag{24}
\end{aligned}$$

in which $|\vec{p}_{\text{irm}}| = |\vec{p}_{q_1\bar{q}_1, q_2\bar{q}_2}|$ and $|\vec{p}_{\text{frm}}| = |\vec{p}_{q_1\bar{q}_4, q_3\bar{q}_2}|$; \hat{p}_{irm} (\hat{p}_{frm}) denotes the polar angles of \vec{p}_{irm} (\vec{p}_{frm}); m_{q_2} and $m_{\bar{q}_2}$ are the q_2 and \bar{q}_2 masses, respectively. The expression of the other transition amplitude $\mathcal{M}_{a\bar{q}_1 \bar{q}_2}$ is similar to the right-hand side in Eq. (24), and is thus given from $\mathcal{M}_{a\bar{q}_1 q_2}$ by replacing $\hat{p}_{q_1\bar{q}_4, q_3\bar{q}_2}$ ($\vec{p}_{q_1\bar{q}_1} + \frac{m_{q_1}}{m_{q_1} + m_{\bar{q}_1}} \vec{p}_{\text{irm}} + \frac{m_{q_1}}{m_{q_1} + m_{\bar{q}_4}} \vec{p}_{\text{frm}}$, $\vec{p}_{q_2\bar{q}_2} + \frac{m_{\bar{q}_2}}{m_{q_2} + m_{\bar{q}_2}} \vec{p}_{\text{irm}} + \frac{m_{\bar{q}_2}}{m_{q_3} + m_{\bar{q}_2}} \vec{p}_{\text{frm}}$, $\vec{p}_{q_2\bar{q}_2} - \vec{p}_{q_1\bar{q}_1} - (\frac{m_{q_2}}{m_{q_2} + m_{\bar{q}_2}} - \frac{m_{\bar{q}_1}}{m_{q_1} + m_{\bar{q}_1}}) \vec{p}_{\text{irm}}$) with $\hat{p}_{q_3\bar{q}_1, q_2\bar{q}_4}$ ($\vec{p}_{q_1\bar{q}_1} - \frac{m_{\bar{q}_1}}{m_{q_1} + m_{\bar{q}_1}} \vec{p}_{\text{irm}} - \frac{m_{\bar{q}_1}}{m_{q_3} + m_{\bar{q}_1}} \vec{p}_{\text{frm}}$, $\vec{p}_{q_2\bar{q}_2} - \frac{m_{q_2}}{m_{q_2} + m_{\bar{q}_2}} \vec{p}_{\text{irm}} - \frac{m_{q_2}}{m_{q_2} + m_{\bar{q}_4}} \vec{p}_{\text{frm}}$, $\vec{p}_{q_1\bar{q}_1} - \vec{p}_{q_2\bar{q}_2} + (\frac{m_{q_1}}{m_{q_1} + m_{\bar{q}_1}} - \frac{m_{\bar{q}_2}}{m_{q_2} + m_{\bar{q}_2}}) \vec{p}_{\text{irm}}$). So far, we have obtained new expressions of the transition amplitudes from Eqs. (2) and (3).

With the transition amplitudes the unpolarized cross section for $A + B \rightarrow C + D$ is

$$\begin{aligned}
\sigma^{\text{unpol}}(\sqrt{s}, T) &= \frac{1}{(2J_A + 1)(2J_B + 1)} \frac{1}{32\pi s} \frac{|\vec{P}'(\sqrt{s})|}{|\vec{P}(\sqrt{s})|} \\
&\times \int_0^\pi d\theta \sum_{J_{Az} J_{Bz} J_{Cz} J_{Dz}} |\mathcal{M}_{a\bar{q}_1 \bar{q}_2} + \mathcal{M}_{a\bar{q}_1 q_2}|^2 \sin \theta, \tag{25}
\end{aligned}$$

where s is the Mandelstam variable obtained from the four-momenta P_A and P_B of mesons A and B by $s = (P_A + P_B)^2$; T is the temperature; J_A (J_B , J_C , J_D) and J_{Az} (J_{Bz} , J_{Cz} , J_{Dz}) of meson A (B , C , D) are the total angular momentum and its z component, respectively; θ is the angle between \vec{P} and \vec{P}' which are the three-dimensional momenta of mesons A and C in the center-of-mass frame, respectively. Let m_A , m_B , m_C , and m_D be the masses of mesons A , B , C , and D , respectively. \vec{P} and \vec{P}' are given by

$$\vec{P}^2(\sqrt{s}) = \frac{1}{4s} \left[(s - m_A^2 - m_B^2)^2 - 4m_A^2 m_B^2 \right], \quad (26)$$

$$\vec{P}'^2(\sqrt{s}) = \frac{1}{4s} \left[(s - m_C^2 - m_D^2)^2 - 4m_C^2 m_D^2 \right]. \quad (27)$$

On the basis of the relativistic energy-momentum relation, we have

$$E_A = \sqrt{\vec{P}^2 + m_A^2} = \frac{1}{2\sqrt{s}}(s + m_A^2 - m_B^2), \quad (28)$$

$$E_B = \sqrt{\vec{P}^2 + m_B^2} = \frac{1}{2\sqrt{s}}(s - m_A^2 + m_B^2), \quad (29)$$

$$E_C = \sqrt{\vec{P}'^2 + m_C^2} = \frac{1}{2\sqrt{s}}(s + m_C^2 - m_D^2), \quad (30)$$

$$E_D = \sqrt{\vec{P}'^2 + m_D^2} = \frac{1}{2\sqrt{s}}(s - m_C^2 + m_D^2). \quad (31)$$

We calculate the cross section in the center-of-mass frame of the two initial mesons. According to the Feynman rules, the two processes $q_1 + \bar{q}_2 \rightarrow q_3 + \bar{q}_4$ and $\bar{q}_1 + q_2 \rightarrow q_3 + \bar{q}_4$ contribute to meson-meson scattering on an equal footing, and the sum $\mathcal{M}_{aq_1\bar{q}_2} + \mathcal{M}_{a\bar{q}_1q_2}$ appears in Eq. (25) if $\mathcal{M}_{aq_1\bar{q}_2} \neq 0$ and $\mathcal{M}_{a\bar{q}_1q_2} \neq 0$.

III. NUMERICAL CROSS SECTIONS AND DISCUSSIONS

The quark-antiquark relative-motion wave functions, $\phi_{A\text{rel}}$ and $\phi_{B\text{rel}}$ in Eq. (4) as well as $\phi_{C\text{rel}}$ and $\phi_{D\text{rel}}$ in Eq. (5), are solutions of the Schrödinger equation with a temperature-dependent quark potential. The potential between constituents a and b in coordinate space is [29]

$$V_{ab}(\vec{r}_{ab}) = -\frac{\vec{\lambda}_a}{2} \cdot \frac{\vec{\lambda}_b}{2} \xi_1 \left[1.3 - \left(\frac{T}{T_c} \right)^4 \right] \tanh(\xi_2 r_{ab}) + \frac{\vec{\lambda}_a}{2} \cdot \frac{\vec{\lambda}_b}{2} \frac{6\pi v(\lambda r_{ab})}{25 r_{ab}} \exp(-\xi_3 r_{ab})$$

$$-\frac{\vec{\lambda}_a}{2} \cdot \frac{\vec{\lambda}_b}{2} \frac{16\pi^2}{25} \frac{d^3}{\pi^{3/2}} \exp(-d^2 r_{ab}^2) \frac{\vec{s}_a \cdot \vec{s}_b}{m_a m_b} + \frac{\vec{\lambda}_a}{2} \cdot \frac{\vec{\lambda}_b}{2} \frac{4\pi}{25} \frac{1}{r_{ab}} \frac{d^2 v(\lambda r_{ab})}{dr_{ab}^2} \frac{\vec{s}_a \cdot \vec{s}_b}{m_a m_b}, \quad (32)$$

where $\xi_1 = 0.525$ GeV, $\xi_2 = 1.5[0.75 + 0.25(T/T_c)^{10}]^6$ GeV, $\xi_3 = 0.6$ GeV, and $\lambda = \sqrt{25/16\pi^2\alpha'}$ with $\alpha' = 1.04$ GeV⁻²; $T_c = 0.175$ GeV is the critical temperature at which the phase transition between the quark-gluon plasma and hadronic matter takes place [33–35]; m_a , \vec{s}_a , and $\vec{\lambda}_a$ are the mass, the spin, and the Gell-Mann matrices for the color generators of constituent a , respectively; the dimensionless function v is given by Buchmüller and Tye in Ref. [36]; the quantity d is related to constituent quark masses by

$$d^2 = d_1^2 \left[\frac{1}{2} + \frac{1}{2} \left(\frac{4m_a m_b}{(m_a + m_b)^2} \right)^4 \right] + d_2^2 \left(\frac{2m_a m_b}{m_a + m_b} \right)^2, \quad (33)$$

where $d_1 = 0.15$ GeV and $d_2 = 0.705$. The potential originates from perturbative quantum chromodynamics (QCD) at short distances and lattice QCD at intermediate and long distances. The first and second terms are the central spin-independent potential of which the short-distance part arises from one-gluon exchange plus perturbative one- and two-loop corrections in vacuum [36] and the intermediate-distance and long-distance part fits well the numerical potential which was obtained in the lattice gauge calculations [33]. The third term is the smeared spin-spin interaction that comes from one-gluon exchange between constituents a and b [37], and the fourth term is the spin-spin interaction that arises from perturbative one- and two-loop corrections to one-gluon exchange [38]. Temperature dependence of the potential is given by the first term, and comes from the lattice gauge calculations [33]. At long distances the spin-independent potential is independent of r_{ab} , and obviously exhibits a plateau at $T/T_c > 0.55$. The plateau height decreases with increasing temperature. Confinement thus becomes weaker and weaker.

The Schrödinger equation with the potential yields energy eigenvalues and quark-antiquark relative-motion wave functions in coordinate space. The sum of the quark mass, the antiquark mass, and an energy eigenvalue gives a meson mass. In the present work we use the constituent quark masses, 0.32 GeV for the up and down quarks and 0.5 GeV for the strange quark. The quark masses are independent of temperature. The experimental masses of π , ρ , K , K^* , η , ω , and ϕ mesons are reproduced from the Schrödinger

equation with the potential at $T = 0$. Furthermore, the temperature dependence of the potential leads to temperature dependence of meson masses and mesonic quark-antiquark relative-motion wave functions. The temperature dependence of the π , ρ , K , and K^* masses are shown in Ref. [39], where the temperature covers the temperature region of hadronic matter, and parametrizations of these meson masses are given. The temperature dependence of the ϕ mass is shown in Ref. [40], and is parametrized as

$$m_\phi = 0.931 \left[1 - \left(\frac{T}{1.12T_c} \right)^{5.46} \right]^{1.32}. \quad (34)$$

Since confinement becomes weaker and weaker with increasing temperature, spatial extension of the mesonic quark-antiquark relative-motion wave functions becomes larger and larger. Since the orbital-angular-momentum quantum numbers of π , ρ , K , K^* , η , ω , and ϕ mesons are zero, the wave functions are not zero at $r_{ab} = 0$. When the temperature increases, the absolute values of the wave functions at $r_{ab} = 0$ decrease.

The transition potentials $V_{aq_1\bar{q}_2}$ and $V_{a\bar{q}_1q_2}$ are derived from perturbative QCD in Ref. [29]. From the wave functions and the transition potentials we get the transition amplitudes $\mathcal{M}_{aq_1\bar{q}_2}$ and $\mathcal{M}_{a\bar{q}_1q_2}$. In practical calculations the summations over L_i and L_f in the transition amplitudes are from 0 to 3. The orbital-angular-momentum quantum numbers L_i and L_f are selected to satisfy that parity is conserved and that the total angular momentum of the two final mesons equals the total angular momentum of the two initial mesons. Values of L_i and L_f are listed in Table 1.

We consider the four $K+\phi$ reactions: $K\phi \rightarrow \pi K$, $K\phi \rightarrow \rho K$, $K\phi \rightarrow \pi K^*$, and $K\phi \rightarrow \rho K^*$. $\mathcal{M}_{aq_1\bar{q}_2}$ and $\mathcal{M}_{a\bar{q}_1q_2}$ are proportional to flavor matrix elements. Since the flavor matrix elements for the $K+\phi$ reactions with total isospin $I = \frac{1}{2}$ are zero for $\mathcal{M}_{aq_1\bar{q}_2}$ and $-\frac{\sqrt{6}}{2}$ for $\mathcal{M}_{a\bar{q}_1q_2}$, only the process $\bar{q}_1 + q_2 \rightarrow q_3 + \bar{q}_4$ contributes to these reactions. The unpolarized cross section for the four $K+\phi$ reactions is

$$\begin{aligned} \sigma^{\text{unpol}}(\sqrt{s}, T) = & \frac{1}{(2J_A + 1)(2J_B + 1)} \frac{1}{32\pi s} \frac{|\vec{P}'(\sqrt{s})|}{|\vec{P}(\sqrt{s})|} \\ & \times \int_0^\pi d\theta \sum_{J_{Az} J_{Bz} J_{Cz} J_{Dz}} |\mathcal{M}_{a\bar{q}_1q_2}|^2 \sin\theta. \end{aligned} \quad (35)$$

If the sum of the masses of the two initial mesons of a reaction is larger than the one

Table 1: Total spin and orbital-angular-momentum quantum number.

reaction	S	S'	L_i	L_f
$K\phi \rightarrow \pi K$	1	0	1	1
	1	0	2	2
	1	0	3	3
$K\phi \rightarrow \rho K$	1	1	0	0,2
	1	1	1	1,3
	1	1	2	0,2
	1	1	3	1,3
$K\phi \rightarrow \pi K^*$	1	1	0	0,2
	1	1	1	1,3
	1	1	2	0,2
	1	1	3	1,3
$K\phi \rightarrow \rho K^*$	1	0	1	1
	1	0	2	2
	1	0	3	3
	1	1	0	0,2
	1	1	1	1,3
	1	1	2	0,2
	1	1	3	1,3
	1	2	0	2
	1	2	1	1,3
	1	2	2	0,2
	1	2	3	1,3

of the two final mesons, the reaction is exothermic. Even slowly-moving initial mesons may start the reaction, and a certain amount of the masses of the initial mesons are converted into kinetic energies of the final mesons. If the sum of the masses of the two initial mesons is smaller than that of the two final mesons, the reaction is endothermic. The initial mesons need kinetic energies to satisfy energy conservation and to start the reaction, and a certain amount of the kinetic energies are converted into the masses of the final mesons.

The reaction $K\phi \rightarrow \rho K^*$ is endothermic at $T/T_c = 0$ and exothermic at $T/T_c = 0.65, 0.75, 0.85, 0.9, \text{ and } 0.95$. The other three reactions are exothermic. Cross sections for exothermic reactions are infinite at threshold energies. We thus start calculations of the cross sections for exothermic reactions at $\sqrt{s} = m_K + m_\phi + 10^{-4} \text{ GeV}$, where m_K and m_ϕ are the masses of the kaon and the ϕ meson, respectively. Numerical unpolarized cross sections for $K\phi \rightarrow \pi K$, $K\phi \rightarrow \rho K$, $K\phi \rightarrow \pi K^*$, and $K\phi \rightarrow \rho K^*$ are plotted as red solid curves in Fig. 1 through Fig. 4. Because the quark potential, the meson masses, and the mesonic quark-antiquark relative-motion wave functions depend on temperature, $|\vec{P}|$, $|\vec{P}'|$, E_A , E_B , E_C , E_D , and $\mathcal{M}_{a\bar{q}_1 q_2}$, which are given in Eq. (24) and Eqs. (26)-(31), depend on temperature. This leads to temperature dependence of the unpolarized cross sections.

The numerical cross sections for endothermic reactions are parametrized as

$$\begin{aligned} \sigma^{\text{unpol}}(\sqrt{s}, T) = & a_1 \left(\frac{\sqrt{s} - \sqrt{s_0}}{b_1} \right)^{c_1} \exp \left[c_1 \left(1 - \frac{\sqrt{s} - \sqrt{s_0}}{b_1} \right) \right] \\ & + a_2 \left(\frac{\sqrt{s} - \sqrt{s_0}}{b_2} \right)^{c_2} \exp \left[c_2 \left(1 - \frac{\sqrt{s} - \sqrt{s_0}}{b_2} \right) \right], \end{aligned} \quad (36)$$

where $\sqrt{s_0}$ is the threshold energy, and a_1 , b_1 , c_1 , a_2 , b_2 , and c_2 are parameters. The numerical cross sections for exothermic reactions are parametrized as

$$\begin{aligned} \sigma^{\text{unpol}}(\sqrt{s}, T) = & \frac{\vec{P}'^2}{\vec{P}^2} \left\{ a_1 \left(\frac{\sqrt{s} - \sqrt{s_0}}{b_1} \right)^{c_1} \exp \left[c_1 \left(1 - \frac{\sqrt{s} - \sqrt{s_0}}{b_1} \right) \right] \right. \\ & \left. + a_2 \left(\frac{\sqrt{s} - \sqrt{s_0}}{b_2} \right)^{c_2} \exp \left[c_2 \left(1 - \frac{\sqrt{s} - \sqrt{s_0}}{b_2} \right) \right] \right\}. \end{aligned} \quad (37)$$

The parameter values are listed in Table 2. d_0 is the separation between the peak's location on the \sqrt{s} -axis and the threshold energy, and $\sqrt{s_z}$ is the square root of the

Mandelstam variable at which the cross section is 1/100 of the peak cross section. For the endothermic reaction $K\phi \rightarrow \rho K^*$ at $T = 0$ a peak is displayed in Fig. 4, and $d_0 = 0.25$ GeV and $\sqrt{s_z} = 3.04$ GeV are obtained from the numerical cross section for $K\phi \rightarrow \rho K^*$. About exothermic reactions we may not see peak cross sections, but \vec{P}^2/\vec{P}'^2 times numerical cross sections for exothermic reactions must show peak cross sections. Hence, for exothermic reactions d_0 and $\sqrt{s_z}$ are obtained from \vec{P}^2/\vec{P}'^2 times the numerical cross sections.

The cross sections given by the parametrizations are plotted as green dashed curves in Fig. 1 through Fig. 4. For the exothermic reactions the solid and dashed curves look coincided. For the endothermic reaction $K\phi \rightarrow \rho K^*$ at $T = 0$, difference between the solid curve and the dashed curve exists around the two peak cross sections and at $\sqrt{s} > 2.2$ GeV.

The threshold energy for each of the exothermic reactions $K\phi \rightarrow \pi K$, $K\phi \rightarrow \rho K$, and $K\phi \rightarrow \pi K^*$ are the sum of the K and ϕ masses. When the temperature increases, decreases of the masses lead to a decrease in the threshold energy as shown in Figs. 1-3. As \sqrt{s} increases near the threshold energy, the cross sections for these reactions decrease rapidly due to the factor $|\vec{P}'|/|\vec{P}|$ in Eq. (35). The threshold energy of the endothermic reaction $K\phi \rightarrow \rho K^*$ at $T = 0$ is the sum of the ρ and K^* masses. As \sqrt{s} increases from the threshold energy, the cross section for $K\phi \rightarrow \rho K^*$ at $T = 0$ increases rapidly from zero, reaches a peak value of about 1.66 mb, and then decreases.

Since the reactions $K\phi \rightarrow \pi K$, $K\phi \rightarrow \rho K$, and $K\phi \rightarrow \pi K^*$ are exothermic, one always find exclusive final states πK , ρK , and πK^* in a $K + \phi$ reaction. However, one may not find the exclusive final state ρK^* in a $K + \phi$ reaction in vacuum, since the reaction $K\phi \rightarrow \rho K^*$ is endothermic at $T = 0$. If the total energy \sqrt{s} of K and ϕ mesons in the center-of-mass frame is smaller than the threshold energy of $K\phi \rightarrow \rho K^*$, the reaction does not occur. If \sqrt{s} is larger than the threshold energy, one can observe ρK^* production.

In hadronic matter with high temperatures the four reactions considered in the present work are exothermic, and always take place. K and ϕ mesons satisfy the Bose-Einstein distribution functions. The reactions and the distribution reduce the ϕ number and affect

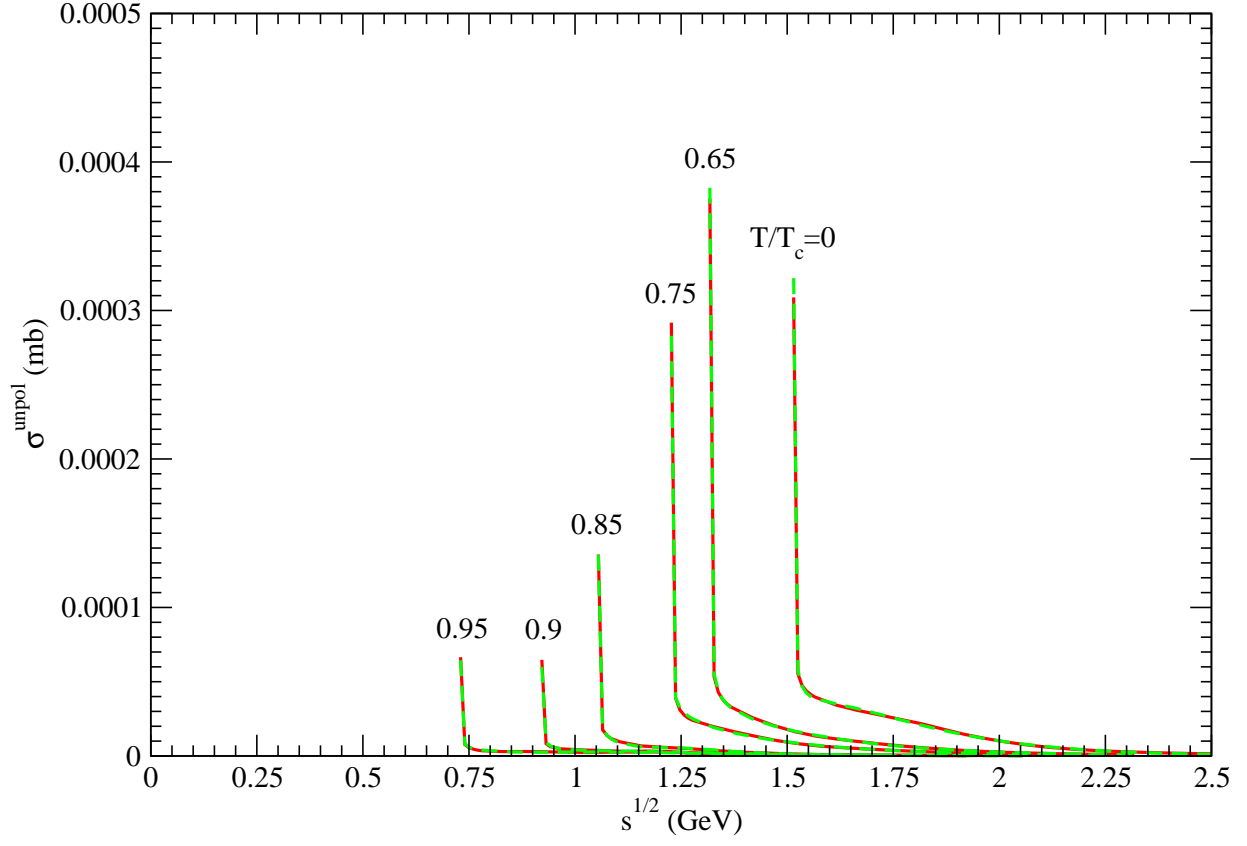


Figure 1: Cross sections for $K\phi \rightarrow \pi K$ at various temperatures. Red solid curves and green dashed curves are obtained from Eq. (35) and Eq. (37), respectively.

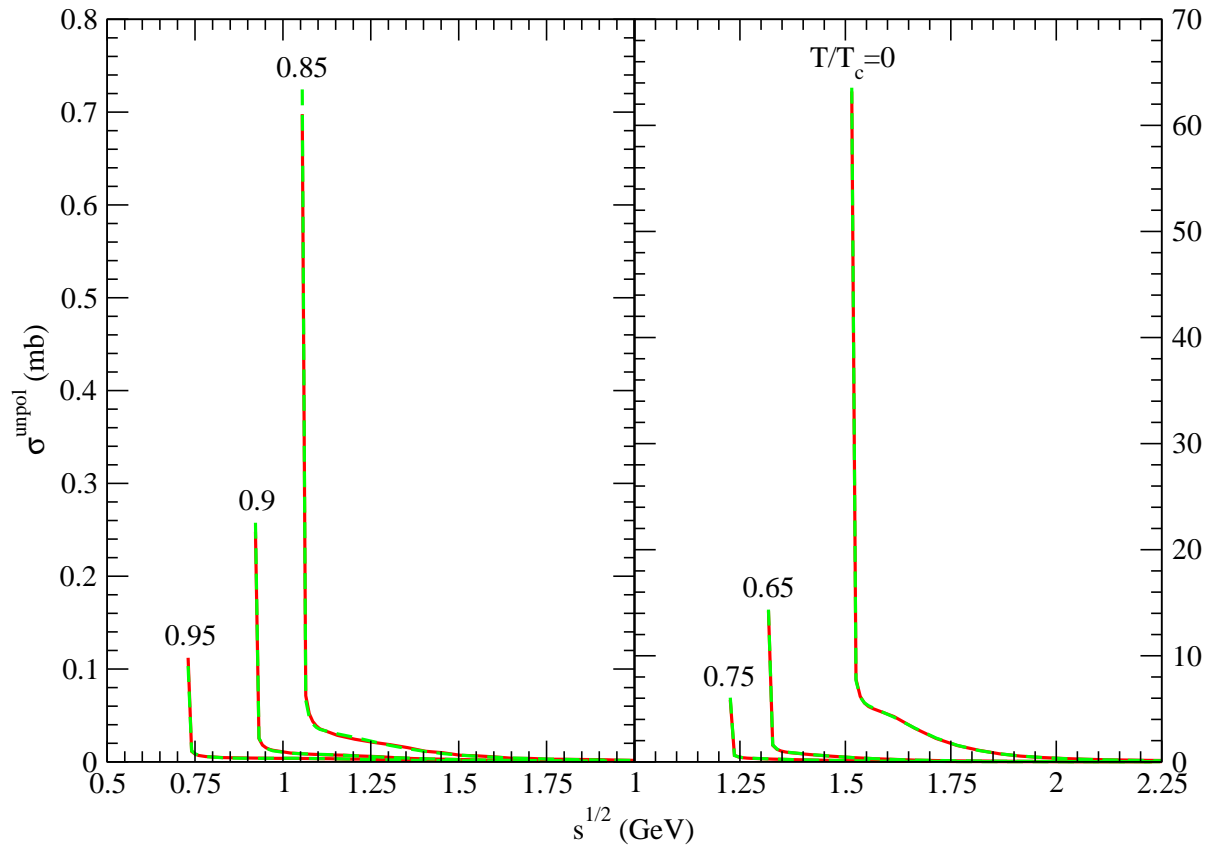


Figure 2: The same as Fig. 1 except for $K\phi \rightarrow \rho K$.

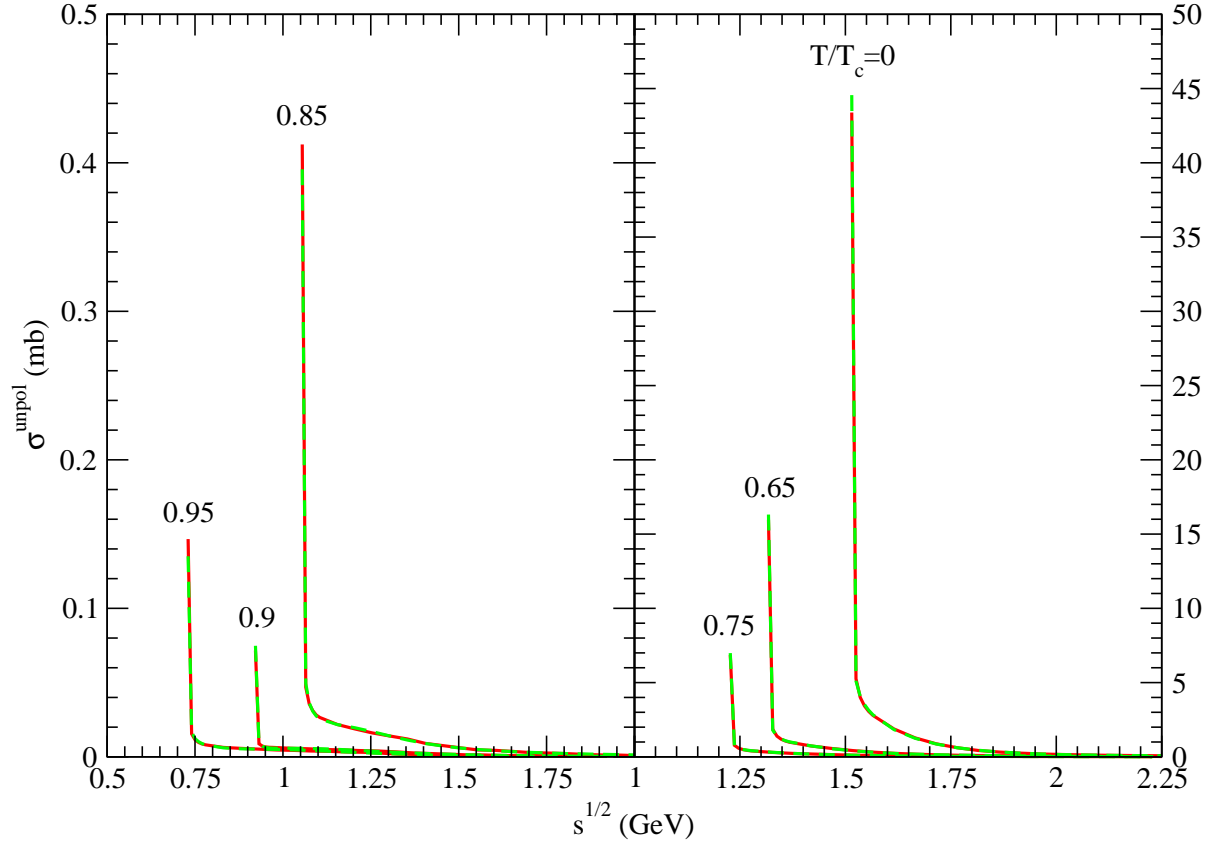


Figure 3: The same as Fig. 1 except for $K\phi \rightarrow \pi K^*$.

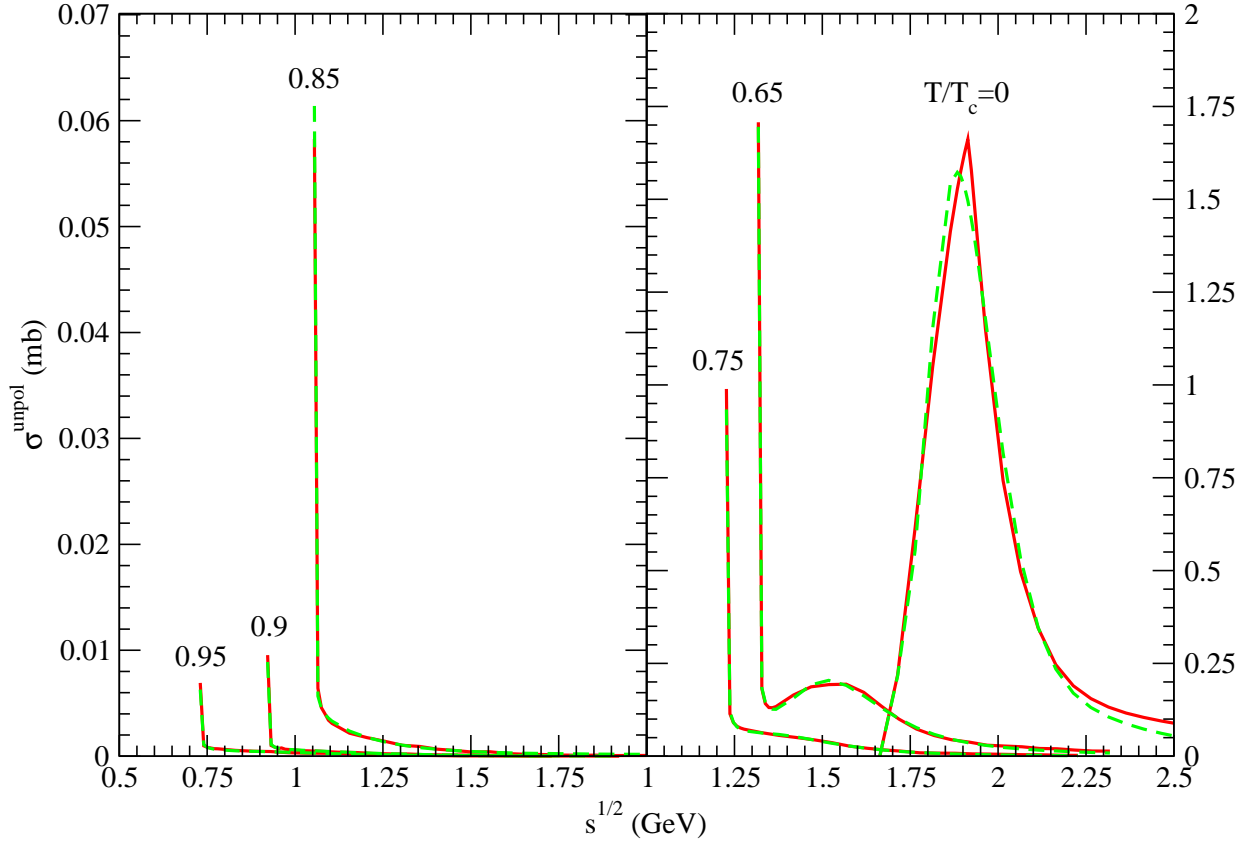


Figure 4: Cross sections for $K\phi \rightarrow \rho K^*$ at various temperatures. Red solid curves and green dashed curves are obtained from Eq. (35) and Eqs. (36)-(37), respectively.

Table 2: Values of the parameters. a_1 and a_2 are in units of millibarns; b_1 , b_2 , d_0 , and $\sqrt{s_z}$ are in units of GeV; c_1 and c_2 are dimensionless.

reaction	T/T_c	a_1	b_1	c_1	a_2	b_2	c_2	d_0	$\sqrt{s_z}$
$K\phi \rightarrow \pi K$	0	0.0000026	0.17	0.62	0.0000046	0.27	1.95	0.3	2.83
	0.65	0.000002	0.13	0.54	0.000003	0.24	1.2	0.15	2.57
	0.75	0.0000002	0.1	0.25	0.0000037	0.19	0.86	0.2	2.46
	0.85	0.00000076	0.239	8.37	0.00000124	0.136	0.58	0.2	2.15
	0.9	0.00000042	0.271	4.7	0.00000094	0.237	0.59	0.3	1.97
	0.95	0.0000008	0.43	5.9	0.0000009	0.23	0.55	0.45	2.17
$K\phi \rightarrow \rho K$	0	0.64	0.125	2.21	0.6	0.107	0.53	0.1	2.87
	0.65	0.11	0.12	0.52	0.07	0.14	2.15	0.15	2.65
	0.75	0.04	0.137	0.49	0.03	0.148	1.93	0.15	1.4
	0.85	0.004	0.183	2.54	0.005	0.167	0.48	0.25	2.81
	0.9	0.00233	0.202	0.5	0.00115	0.2582	4.2	0.25	2.2
	0.95	0.0009	0.371	6.63	0.0014	0.258	0.53	0.4	3.52
$K\phi \rightarrow \pi K^*$	0	0.1	0.153	0.34	0.33	0.096	0.95	0.1	2.94
	0.65	0.121	0.132	0.51	0.068	0.121	1.84	0.15	2.69
	0.75	0.05	0.147	0.5	0.027	0.127	1.65	0.15	2.52
	0.85	0.0025	0.2	3.4	0.0044	0.18	0.55	0.2	2.14
	0.9	0.00089	0.211	0.54	0.00145	0.256	2.24	0.35	2.27
	0.95	0.0014	0.358	3.9	0.0016	0.153	0.55	0.3	1.86
$K\phi \rightarrow \rho K^*$	0	0.29	0.17	0.72	1.29	0.22	6.18	0.25	3.04
	0.65	0.062	0.14	0.49	0.096	0.226	3.9	0.25	4.19
	0.75	0.013	0.202	3.04	0.019	0.123	0.55	0.2	2.48
	0.85	0.00018	0.34	0.28	0.00059	0.11	0.91	0.15	2.16
	0.9	0.000087	0.199	1.86	0.000105	0.153	0.54	0.25	1.48
	0.95	0.00007	0.26	2.7	0.00013	0.17	0.62	0.2	18.02

the ϕ momentum spectra and the ϕ nuclear modification factor, which are observed in ultrarelativistic heavy-ion collisions [3, 6, 13].

The total spin of the two initial mesons in the reaction $K\phi \rightarrow \pi K$ is 1, and the total spin of the two final mesons is 0. Because the two total spins are unequal, the cross section for $K\phi \rightarrow \pi K$ is very small. About $K\phi \rightarrow \rho K$, $K\phi \rightarrow \pi K^*$, and $K\phi \rightarrow \rho K^*$ the total spin of the two initial mesons may equal the one of the two final mesons, and the cross sections may be a few millibarns when \sqrt{s} is not at the threshold energy.

IV. SUMMARY

With the development in spherical harmonics of the relative-motion wave functions of the two initial mesons and of the two final mesons, new expressions of the transition amplitudes have been obtained. With the transition amplitudes we have calculated unpolarized cross sections for $K\phi \rightarrow \pi K$, $K\phi \rightarrow \rho K$, $K\phi \rightarrow \pi K^*$, and $K\phi \rightarrow \rho K^*$, which are governed by quark-antiquark annihilation and creation. Both parity conservation and total-angular-momentum conservation are maintained. To use the numerical cross sections conveniently, we have parametrized the cross sections. Each of the exothermic reactions $K\phi \rightarrow \pi K$, $K\phi \rightarrow \rho K$, and $K\phi \rightarrow \pi K^*$ exhibits a rapid decrease first and then a slow decrease in cross section with increasing \sqrt{s} from the threshold energy. That the reaction $K\phi \rightarrow \rho K^*$ is endothermic or exothermic depends on temperature. The temperature-dependent cross sections are related to temperature dependence of the quark potential, the quark-antiquark relative-motion wave functions, and the meson masses.

ACKNOWLEDGEMENTS

This work was supported by the National Natural Science Foundation of China under Grant No. 11175111.

References

- [1] J. Rafelski and B. Müller, Phys. Rev. Lett. 48, 1066 (1982).

- [2] A. Shor, Phys. Rev. Lett. 54, 1122 (1985).
- [3] B. I. Abelev *et al.*, Phys. Rev. Lett. 99, 112301 (2007).
- [4] B. I. Abelev *et al.*, Phys. Lett. B 673, 183 (2009).
- [5] B. I. Abelev *et al.*, Phys. Rev. C 79, 064903 (2009).
- [6] A. Adare *et al.*, Phys. Rev. C 83, 024909 (2011).
- [7] L. Adamczyk *et al.*, Phys. Rev. C 88, 014902 (2013).
- [8] L. Adamczyk *et al.*, Phys. Rev. C 93, 021903(R) (2016).
- [9] J. Adam *et al.*, Phys. Rev. C 102, 034909 (2020).
- [10] M. S. Abdallah *et al.*, Phys. Rev. C 105, 064911 (2022).
- [11] N. J. Abdulameer *et al.*, Phys. Rev. C 107, 014907 (2023).
- [12] B. Abelev *et al.*, Phys. Rev. C 91, 024609 (2015).
- [13] J. Adam *et al.*, Phys. Rev. C 95, 064606 (2017).
- [14] S. Acharya *et al.*, Phys. Lett. B 802, 135225 (2020).
- [15] S. Acharya *et al.*, Phys. Rev. C 106, 034907 (2022).
- [16] P.-Z. Bi and J. Rafelski, Phys. Lett. B 262, 485 (1991).
- [17] C. M. Ko and D. Seibert, Phys. Rev. C 49, 2198 (1994).
- [18] K. Haglin, Nucl. Phys. A 584, 719 (1995).
- [19] W. Smith and K. L. Haglin, Phys. Rev. C 57, 1449 (1998).
- [20] W. S. Chung, G. Q. Li, and C. M. Ko, Nucl. Phys. A 625, 347 (1997).
- [21] L. Alvarez-Ruso and V. Koch, Phys. Rev. C 65, 054901 (2002).

- [22] A. Martínez Torres, K. P. Khemchandani, L. M. Abreu, F. S. Navarra, and M. Nielsen, Phys. Rev. D 97, 056001 (2018).
- [23] Z.-F. Luo and X.-M. Xu, Chin. Phys. C 36, 836 (2012).
- [24] X.-M. Xu and H. J. Weber, Mod. Phys. Lett. A 35, 2030016 (2020).
- [25] X. Qian *et al.*, Phys. Lett. B 680, 417 (2009).
- [26] J. Adamczewski-Musch *et al.*, Phys. Rev. Lett. 123, 022002 (2019).
- [27] T. Barnes and E. S. Swanson, Phys. Rev. D 46, 131 (1992).
- [28] E. S. Swanson, Ann. Phys. (N.Y.) 220, 73 (1992).
- [29] Z.-Y. Shen, X.-M. Xu, and H. J. Weber, Phys. Rev. D 94, 034030 (2016).
- [30] T.-T. Wang and X.-M. Xu, Chin. Phys. C 43, 024102 (2019).
- [31] G. B. Arfken and H. J. Weber, *Mathematical Methods for Physicists* (Elsevier, Amsterdam, 2006).
- [32] C. J. Joachain, *Quantum Collision Theory* (North-Holland Publishing Company, Amsterdam, 1983).
- [33] F. Karsch, E. Laermann, and A. Peikert, Nucl. Phys. B 605, 579 (2001).
- [34] S. Digal, P. Petreczky, and H. Satz, Phys. Lett. B 514, 57 (2001).
- [35] X.-M. Xu, C.-Y. Wong, and T. Barnes, Phys. Rev. C 67, 014907 (2003).
- [36] W. Buchmüller and S.-H. H. Tye, Phys. Rev. D 24, 132 (1981).
- [37] S. Godfrey and N. Isgur, Phys. Rev. D 32, 189 (1985).
- [38] X.-M. Xu, Nucl. Phys. A 697, 825 (2002).
- [39] Z.-Y. Shen and X.-M. Xu, J. Korean Phys. Soc. 66, 754 (2015).
- [40] W.-X. Li, X.-M. Xu, and H. J. Weber, Eur. Phys. J. C 81, 225 (2021).